

Abstract

Abstracts do not include sources, but are here for the purpose of notes.)

The physical processes that creates electrical signals in neurons are well understood, but how the signals are processed into actions and thoughts has yet to receive a scientifically robust answer (add more sources) [9]. Cell type classification is of high importance because the function of different neurons is still largely a mystery.

Contents

1	Introduction	5
2	Theory	7
2.1	The Neuron	7
2.2	Electrical Activity	8
2.3	Action Potential	9
2.4	Neuron Models	9
2.5	Electrodes	9
2.6	Calculating Extracellular Potential	9
2.7	Neuron & LFPy	10
3	Methods	13
3.1	Pettersen & Einevoll (2008) Reproduction	13
3.2	Blue Brain	16
3.3	Spike Width Measurement	16
3.4	Simulations with LFPyUtil	17
4	Results	19
5	Discussion	21
A	Appendix	23
A.1	Quasistatic Approximation in Neural Tissue	23
	Bibliography	25

1 | Introduction

Introduce the topic, the problem and how the problem is being solved.

Since the conception of neuroscience the neurons function have been studied on many levels and with many perspectives, from a single neuron level to networks of neurons with chemistry, physics, medicine and psychology to name some.

2 | Theory

2.1	The Neuron	7
2.2	Electrical Activity	8
2.3	Action Potential	9
2.4	Neuron Models	9
2.5	Electrodes	9
2.6	Calculating Extracellular Potential	9
2.7	Neuron & LFPy	10

2.1 The Neuron

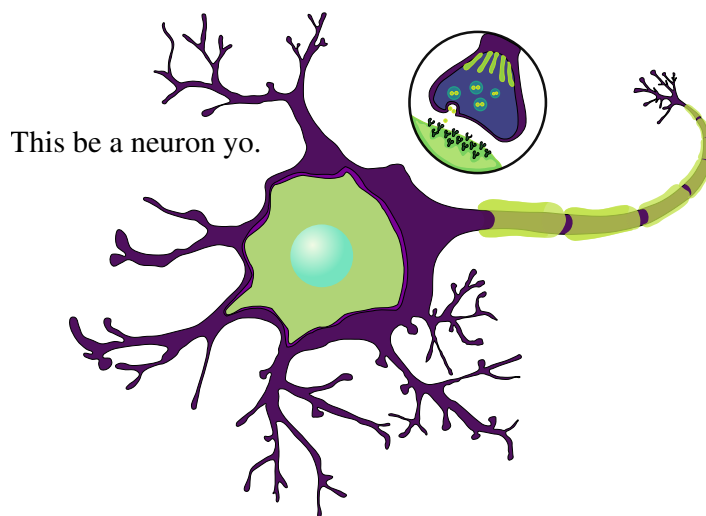


Figure 2.1: Stuff about this neuron.

Neurons are a fundamental part of all brain functions and are electrically excitable brain cells. Other names include **nerve cells**, **neurone** or more colloquially **brain cells**.

The body of the neuron, the **soma**, has **dendrites** and the **axon** attached to it. The dendrites and the axon are very thin branching structures with a width usually in the order of $1\mu\text{m}$. While neurons often have many dendrites directly attached to the soma there is only one axon attached through the **axon hillock**. The axon can branch several times before it ends and usually connects to the dendrites of other neurons via synapses. The synapses are electrically sensitive which allows information to pass between neurons. Though the majority of all synapses are

axo-dendritic (axon to dendrite), other junctions are also possible. Other junctions include but are not limited to, dendrite to dendrite, axon to axon and axon to blood vessel.

Because of properties with the cell membrane the neuron can fire action potentials when it is electrically excited. These action potentials are sharp voltage changes that propagate through the full structure of the neuron. The same properties that makes the neuron able to fire makes the action potential **regenerative**, meaning it will propagate without decaying.

2.2 Electrical Activity

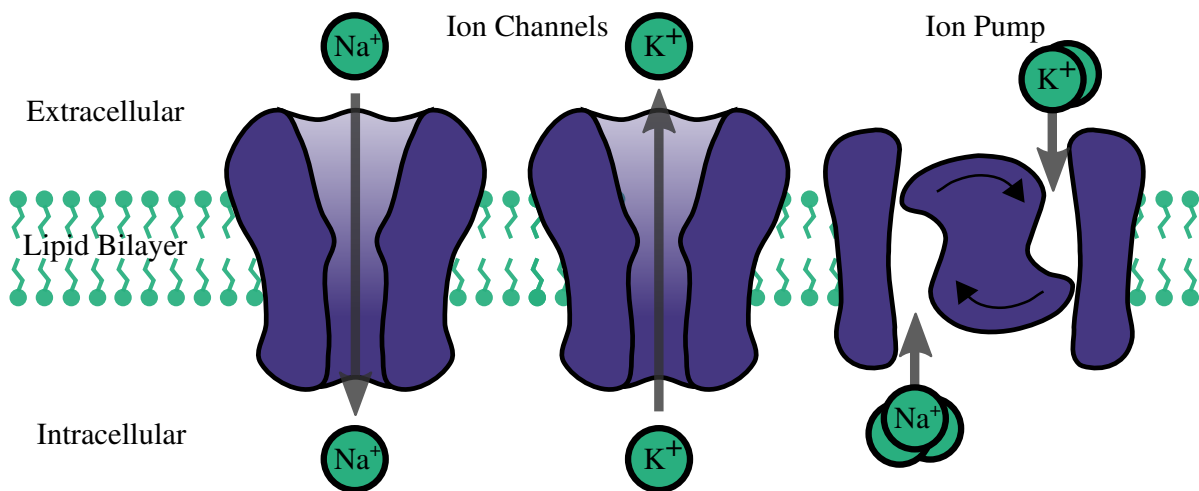


Figure 2.2: Stuff about this neuron.

The electrical activity of neurons are caused by different concentrations of ions in the extracellular and intracellular medium. The cell membrane consists of a 5 nm lipid bilayer which is impenetrable to ions. In the membrane sits different **ion channels** and **ion pumps** which can have selective permeability to ions, this creates a potential gradient across the membrane. The most significant ions in this process are Sodium (Na^+), Potassium (K^+), Calcium (Ca^{2+}), Magnesium (Mg^{2+}) and Chloride (Cl^-). Ion channels are divided between passive channels and active channels where the active can change permeability under certain conditions while passive channels have a constant permeability.

The ion pumps differ from the channels by actively transporting certain ions through the membrane. For instance, the Sodium-Potassium exchanger pushes two Na^+ ions out of the cell for every three K^+ it pushes into the cell. Doing this creates a net loss of charge inside the cell and the pump is therefore electrogenic. Not all pumps are electrogenic, the Sodium-Hydrogen exchanger transports H^+ and Na^+ without effecting the net charge. For each H^+ ion out of the cell the pump pushes one Na^+ into the cell.

Hodgkin & Huxley [5], Connor & Stevens [1], and Sterratt et al. [9]

2.3 Action Potential

Action potentials are sharp increases in the membrane potential followed by a less sharp decrease towards the resting potential. In the depolarization phase the potential rises towards the peak magnitude, while in the repolarization phase the potential decreases towards the cells resting potential. When the potential is below the resting potential it reaches the afterhyperpolarization phase before it returns to its resting potential.

2.4 Neuron Models

There are multiple models for neurons, some of the main groups are point models and compartmental models. List many models? Multi-compartmental models can be useful to understand the processing of neurons with complex morphological structures

2.5 Electrodes

2.6 Calculating Extracellular Potential

The extracellular potential is the electric potential generated from the transmembrane currents in the neurons. When a neuron fires this can be seen from the extracellular potential which will have a spike which is similar to the intracellular spike.

By modelling the neuron as compartments and approximating each compartment as a spherical volume current source at position \mathbf{r}_0 , the potential at position \mathbf{r} at time t will be,

$$\mathbf{E}(\mathbf{r}, t) = \frac{1}{4\pi\sigma} \frac{I_0(t)}{|\mathbf{r} - \mathbf{r}_0|} \quad (2.1)$$

$$\mathbf{E}(\mathbf{r}, t) = \sum_{n=1}^N \frac{1}{4\pi\sigma} \frac{I_n(t)}{|\mathbf{r} - \mathbf{r}_0|} \quad (2.2)$$

Potential from compartments modelled as line sources.

$$\mathbf{E}(\mathbf{r}, t) = \frac{1}{4\pi\sigma} \sum_{n=1}^N I_n(t) \frac{dr_n}{|\mathbf{r} - \mathbf{r}_0|} \quad (2.3)$$

$$= \frac{1}{4\pi\sigma} \sum_{n=1}^N I_n(t) \frac{1}{\Delta s_n} \log \left| \frac{\sqrt{h_n^2 + \rho_n^2} - h_n}{\sqrt{l_n^2 + \rho_n^2} - l_n} \right| \quad (2.4)$$

Taken from [Lindén et al. \[6\]](#)

This equation rests on two assumptions,

1. The permeability μ of the extracellular medium is the same as that of vacuum μ_0 .

2. The quasistatic approximation which lets the time derivatives, $\partial E/\partial t$, be ignored as source terms. See [appendix A.1](#)

The extracellular potential can be calculated using Maxwell's equations and the continuity equation if the spatial distribution (morphology) of transmembrane currents and the extracellular conductivity is known.

In the quasistatic approximation, since $\nabla \times \mathbf{E} = 0$, the electric field can be expressed with a scalar potential.

Forward problem = calculate the potential from the current source, inverse problem is used in magnetoencephalography (important). The amplitude of a spike in the extracellular potential is usually in the magnitude of $< 200\mu\text{V}$. The noise of electrodes vary, but can be as much as $20\mu\text{V}$. This limits the range electrodes can record from.

The currents sum to zero, while the spike is very visible, there are many small currents in the dendrites with opposite current. ([4])

The extracellular spike width tend to increase with distance from soma because of the neuronal morphology. This article used a passive neuron model with different morphologies to show that the spike width increases with distance to soma. The spike amplitude also decreases with distance to soma and seems to follow a power law. ([8]).

The shape of extracellular spikes are mainly dependent on the membrane currents and the morphology of the cell. Some of the effects from the morphology of the cell are increased spike width and decreased amplitude from distance to soma.

Many things here from around page 245. When the conductivity σ and the current generators are known, Maxwell's equations and the continuity equation can be used to calculate the electric field E and magnetic field B . (TODO: Copied text) ([4])

Background

Recording is usually done using electrodes, this makes recording the membrane potential more challenging than recording from the extracellular medium as the electrode has to be very close or inside the cell. At the time of writing, recording the membrane potential of a conscious subject is nearly impossible, this makes understanding extracellular potentials vital for current research.

Early calculations was done by Rall 1962 investigating the interaction between action potentials and synapses using cylinders as the current source. (TODO: Read article, make more understandable.) Holt and Koch 1999 added compartmental models to reconstruct pyramidal neurons.

The information about the transmembrane current is usually difficult to obtain, as well as the morphology.

2.7 Neuron & LFPy

LFPy is a Python module that uses Neuron and the mentioned methods to calculate the electric field outside the neuron. [6]

Background

3 | Methods

3.1	Pettersen & Einevoll (2008) Reproduction	13
3.1.1	Simulation	13
3.1.2	Results	14
3.1.3	Discussion	16
3.2	Blue Brain	16
3.3	Spike Width Measurement	16
3.4	Simulations with LFPyUtil	17
A.1	Quasistatic Approximation in Neural Tissue	23

3.1 Pettersen & Einevoll (2008) Reproduction

To verify that the simulation environment could be trusted some results from [Pettersen & Einevoll \[8\]](#) was replicated. Specifically the spike width and amplitude dependency in relation to the distance from soma was compared to current results.

3.1.1 Simulation

Cell: The [Mainen & Sejnowski \[7\]](#) cell was used with a passive model, which is the same model used in [Pettersen & Einevoll \[8\]](#). It is not clear in which plane the measurements was taken from so the cell was rotated using PCA (principal component analysis) on the compartment positions. This rotates the cell so most of the dendrites are along the y and x-axis.

Spike Generation: An action potential was generated using the Connor-Stevens model [\[1, 2\]](#) using the same parameters as [Dayan & Abbott \[3\]](#). This had an amplitude of $107.6mV$ from baseline with the peak at $48.21mV$. These values are similar (TODO: how similar?) to [Dayan & Abbott \[3\]](#), but not with [Pettersen & Einevoll \[8\]](#) which had an amplitude of $83mV$ from baseline. To compensate for the difference the action potential was normalized to $83mV$ manually ([fig. 3.1](#)).

Parameters: Parameters are the same as [Pettersen & Einevoll \[8\]](#) and [Dayan & Abbott \[3\]](#). Membrane resistance $R_m = 3 \cdot 10^4 \Omega/cm^2$, membrane capacitance $C_m = 1\mu F/cm^2$, axial resistance $R_a = 150 \Omega/cm^2$, time resolution $dt = 2^{-6}ms$. The reversal potential was set to zero. The action potential was imposed in all soma sections using the "play" vector function in Neuron.

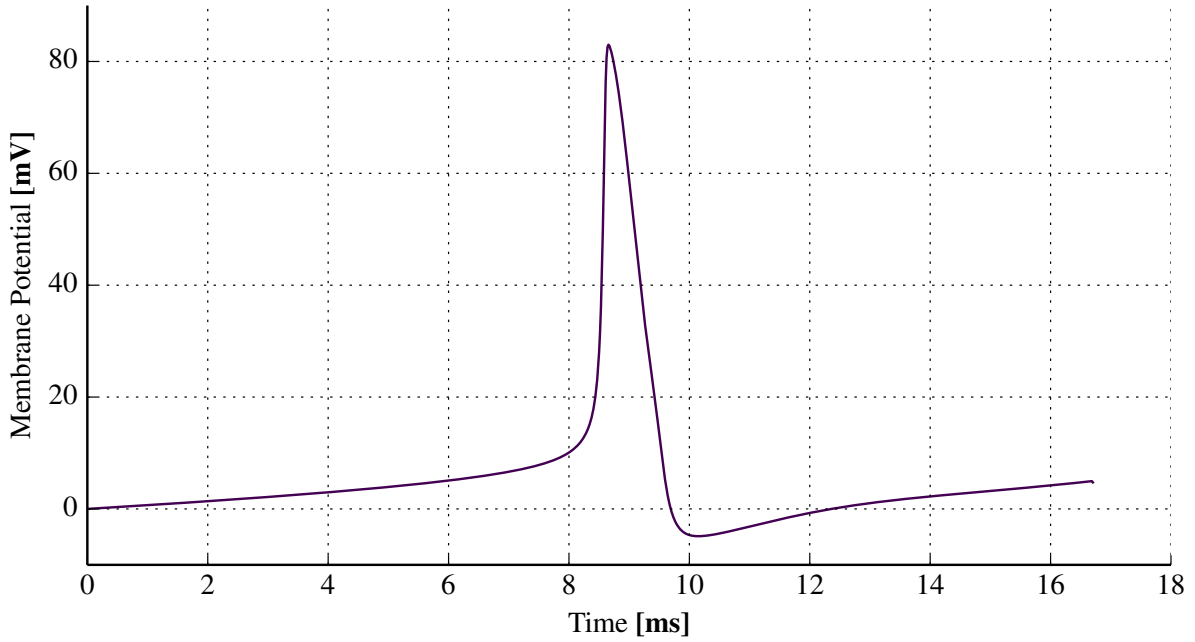


Figure 3.1: Soma membrane voltage.

Electrode Positions: Recording sites were placed in the xz plane at 11 linearly spaced positions along 36 lines with equal angular spacing. (TODO: Show the electrode positions.)

Spike Width & Amplitude: A baseline was set as the value at the start of the signal. Amplitude was calculated as the difference between maximum absolute value and the baseline. The spike width was calculated at half width at maximum amplitude.

Spike width was recorded at $0.5625ms$ for $dt = 2 \cdot 10^{-5}$, similar to $0.55ms$ from [Pettersen & Einevoll \[8\]](#). When increasing the resolution to $dt = 2 \cdot 10^{-6}ms$ the spike width rose to $0.625ms$.

3.1.2 Results

The action potential that was used in [Pettersen & Einevoll \[8\]](#) is similar to the one used here. The amplitude of the fourier transform is displayed in [fig. 3.2](#), which is in close resemblance to the standard action potential in Fig. 3 in the paper.

The spike width increases with the distance from soma as seen in [fig. 3.3](#). These results are lower than the widths reported in [Pettersen & Einevoll \[8\]](#). (Use more time on editing the Connor-Stevens model to come closer to an max.amplitude on $20mV$?).

Sudden changes in spike width was experienced with increased distance from soma. Above $200\mu V$ the spikes shapes are not well defined. This was also reported in [Pettersen & Einevoll \[8\]](#).

[Pettersen & Einevoll \[8\]](#) reports a spike amplitude above $150\mu V$ at $20\mu m$, this does not match current findings. [fig. 3.4](#) shows spike amplitude with logarithmic axes. (TODO: Is numbers on the power law decays necessary?) Although the data does not match [Pettersen & Einevoll \[8\]](#), it is comparable with what is expected in the near and far limit field of a ball and

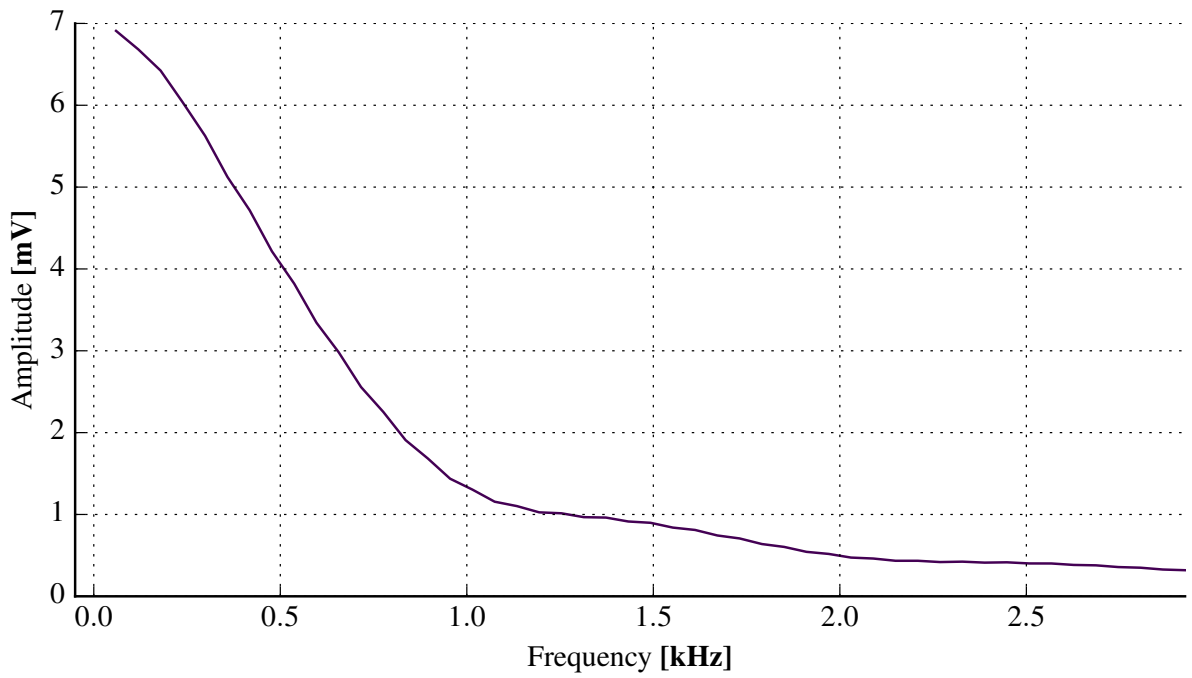


Figure 3.2: Frequency spectrum of simulated somatic membrane potential.

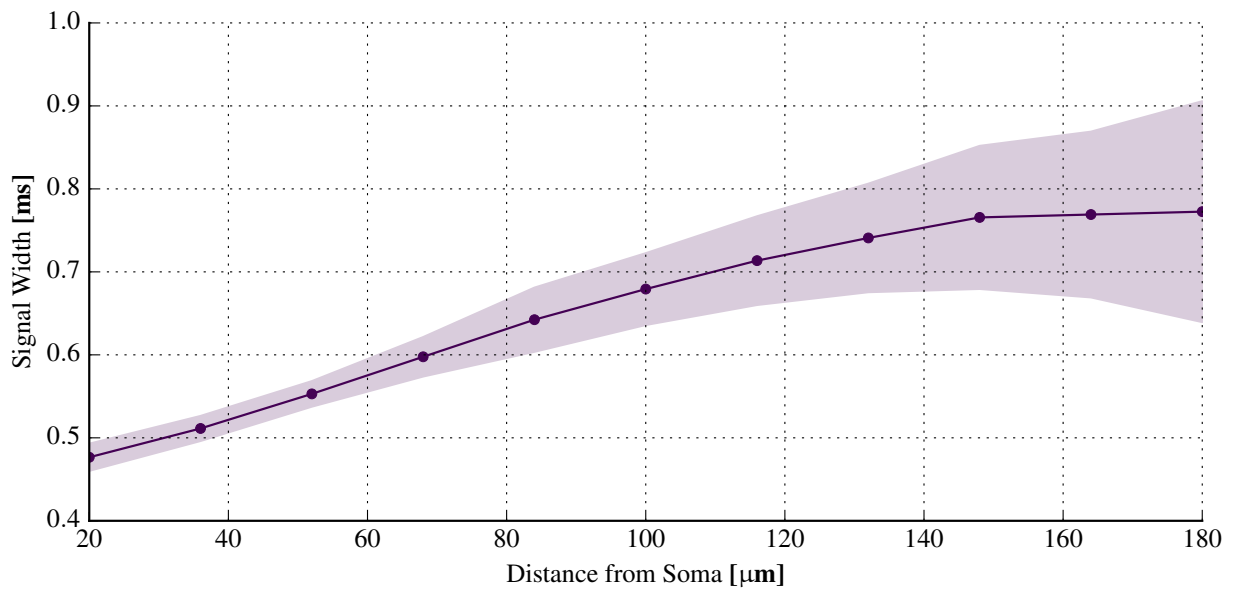


Figure 3.3: Spike width over distance. Mean \pm 1 std.

stick neuron. In the near field the expectation is a $1/r$ decay and in the far field it is $1/r^2$ or $1/r^3$ depending on distance. (TODO: Clarify this, put reference back to theory chapter.)

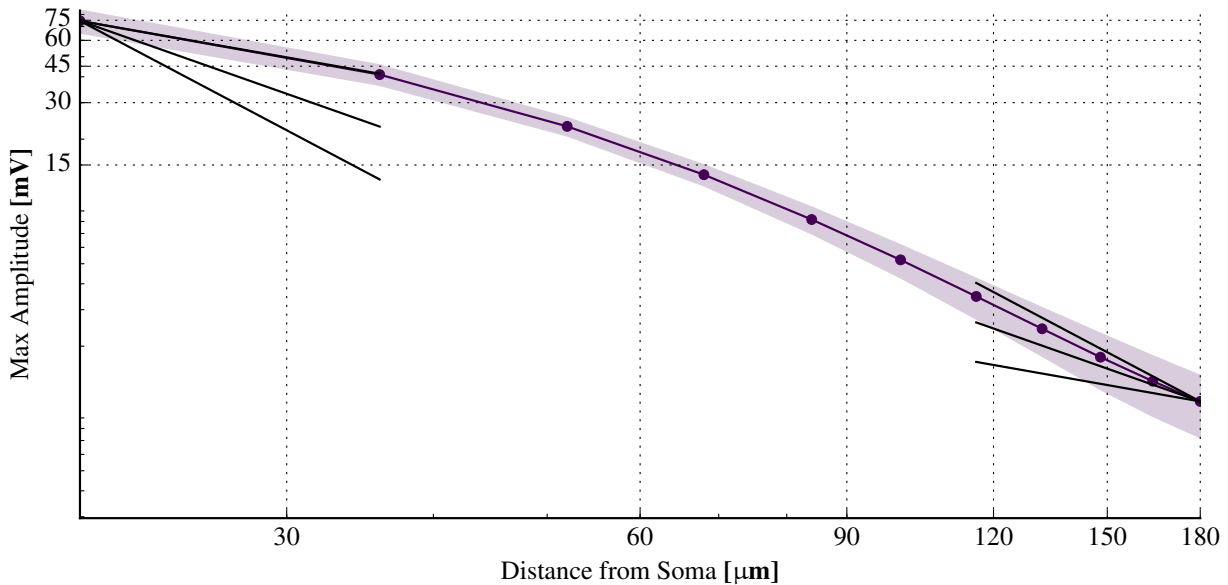


Figure 3.4: Spike amplitude over distance. Mean \pm 1 std. The power law decays $1/r$, $1/r^2$ and $1/r^3$ are shown at the leftmost and rightmost data points.

3.1.3 Discussion

3.2 Blue Brain

The Blue Brain project released XXX models based upon neurons from the hind-limb somatosensory cortex from 2-week-old Wistar Han rats. The models were used The extracellular potential was calculated using "TODO: Insert parameters here".

Use the models. Write code to capture one action potential. Bursting neurons often have adapting action potential, what to do there.

3.3 Spike Width Measurement

Many different definitions of spike width have been used to differentiate neurons, but to date it is not clear which definition is best suited for neuron classification.

Width Type I - Peak-to-peak:

Width is measured as the time from the minimum potential to the maximum. This is the time from the polarization phase to the afterhyperpolarization phase.

Width Type II - Width at Half Amplitude:

Width is measured as the duration the spike is below half amplitude of the signal measured from the baseline at the start of the signal.

Width Type II - Width at Half Amplitude:

Width is measured as the duration the spike is below half amplitude of the signal measured from the baseline at the start of the signal.

3.4 Simulations with LFPyUtil

LFPyUtil is a python package that was created for this project with the purpose of simplifying the simulation pipeline for multiple neurons and creating an easy to use interface when developing new simulations.

In all simulations the extracellular conductivity was set to $\sigma = 0.3 \Omega \text{ m}$ based upon data from experimental measurements.

All stimulus electrodes use the `LFPy.StimIntElectrode` with a custom made electrode named `ISyn`. With the default stimulus all transmembrane currents will be summed equal the input current, using `ISyn` prevents this and the currents are correctly summed to 0.

The following items are python objects in LFPyUtil.

SphereRand

`SphereRand` places electrodes placed in uniformly distributed locations around the soma within a default radius of $50 \mu\text{m}$. Spike timing is detected by thresholding the soma membrane potential. That timing is applied to all electrodes such that all electrodes measure the same part of the simulation. If the signal has several spikes the spike index must be supplied, the default setting uses the first spike.

4 | Results

In figure ?? the spike width from interneurons and pyramidal neurons have been plottet seperatly. Neurons in the pyramidal group are the type TTPC1 and TTPC2 The groups suggests that interneuron can be seperated from pyramidal neurons depending on their spike shape.

5 | Discussion

Nothing here yet.

A | Appendix

A.1 Quasistatic Approximation in Neural Tissue

A quasistatic approximation implies that the equations have a form that does not include time derivatives (static). Some quantities can be allowed to vary over time, but slowly. Here we show that the quasistatic approximation is a valid assumption in neural tissue. First start with Maxwell's equations.

$$\begin{aligned}\nabla \cdot \mathbf{E} &= \rho/e \\ \nabla \times \mathbf{E} &= -\partial \mathbf{B} / \partial t\end{aligned}\tag{A.1}$$

$$\begin{aligned}\nabla \cdot \mathbf{B} &= 0 \\ \nabla \times \mathbf{B} &= \mu_0(\mathbf{J} + \epsilon_0 \partial \mathbf{E} / \partial t)\end{aligned}\tag{A.2}$$

In a passive nonmagnetic medium, \mathbf{J} is the sum of ohmic volume current and the polarization current

$$\mathbf{J} = \sigma \mathbf{E} + \partial \mathbf{P} / \partial t\tag{A.3}$$

where $\mathbf{P} = (\epsilon - \epsilon_0)\mathbf{E}$ is the polarization and ϵ is the permittivity of the material. In neuromagnetism, we generally deal with frequencies that are below 100 Hz. Cellular electrical phenomena contain mostly frequencies below 1 kHz. Let σ and ϵ be uniform and let us consider electromagnetic wave at frequency f .

$$\mathbf{E} = \mathbf{E}_0(\mathbf{r}) \exp(i2\pi f t)\tag{A.4}$$

With eqs. (A.2) and (A.3) we get,

$$\nabla \times \mathbf{B} = \mu_0(\sigma \mathbf{E} + (\epsilon - \epsilon_0) \partial \mathbf{E} / \partial t + \epsilon_0 \partial \mathbf{E} / \partial t)\tag{A.5}$$

For the quasistatic approximation to be valid, it is necessary that the time-derivative terms be small compared to the ohmic current.

$$|\epsilon \mathbf{E} / \partial t| \ll |\sigma \mathbf{E}| \rightarrow 2\pi f \epsilon / \sigma \ll 1\tag{A.6}$$

With $\sigma = 0.3 \Omega^{-1} \text{ m}^{-1}$, the value of brain tissue, $\epsilon = 10^5 \cdot \epsilon_0$, and $f = 100 \text{ Hz}$, we find

$$2\pi f \epsilon / \sigma = 2 \cdot 10^{-3} \ll 1\tag{A.7}$$

In addition, $\partial \mathbf{B} / \partial t$ must be small. from eqs. (A.1) and (A.2) ,

$$\begin{aligned}
\nabla \times \nabla \times \mathbf{E} &= -\frac{\partial}{\partial t}(\nabla \times \mathbf{B}) \\
&= -\mu_0 \frac{\partial}{\partial t}(\sigma \mathbf{E} + \epsilon \partial \mathbf{E} / \partial t) \\
&= -i2\pi f \mu_0 (\sigma + i2\pi f \epsilon) \mathbf{E}
\end{aligned} \tag{A.8}$$

Solutions of this equation have spatial changes on the characteristic length scale

$$\lambda_c = |2\pi f \mu_0 \sigma (1 + i2\pi f \epsilon / \sigma)|^{-1/2} \approx 65 \text{ m} \tag{A.9}$$

This length is much longer than the diameter of the head. This implies that the contribution of $\partial \mathbf{B} / \partial t$ to \mathbf{E} is small. Therefore, the quasistatic approximation appears justified. This does not mean that we should forget time-dependent phenomena altogether. For example, the capacitive current through the cell membrane is significant in determining the properties of the action potential. Nevertheless, this so-called displacement current, $\epsilon_0 \partial \mathbf{E} / \partial t$, need not be taken into account in the calculation of \mathbf{B} .

Copied from [Hämäläinen et al. \[4\]](#)

Bibliography

- [1] J. A. Connor & C. F. Stevens. “Prediction of repetitive firing behaviour from voltage clamp data on an isolated neurone soma.” In: [The Journal of Physiology](#) 213.1 (1971). 00704, pp. 31–53.
- [2] J. A. Connor, D. Walter, & R. McKown. “Neural repetitive firing: modifications of the Hodgkin-Huxley axon suggested by experimental results from crustacean axons.” In: [Biophysical Journal](#) 18.1 (1977). 00236, pp. 81–102.
- [3] Peter Dayan & Laurence F. Abbott. [Theoretical neuroscience](#). Vol. 806. 03314. Cambridge, MA: MIT Press, 2001.
- [4] Matti Hämäläinen et al. “Magnetoencephalography- theory, instrumentation, and applications to noninvasive studies of the working human brain.” In: [Reviews of modern Physics](#) 65.2 (1993). 03322, p. 413.
- [5] Alan L. Hodgkin & Andrew F. Huxley. “A quantitative description of membrane current and its application to conduction and excitation in nerve.” In: [The Journal of physiology](#) 117.4 (1952). 16698, pp. 500–544.
- [6] Henrik Lindén et al. “LFPy: a tool for biophysical simulation of extracellular potentials generated by detailed model neurons.” In: [Frontiers in neuroinformatics](#) 7 (2013). 00015.
- [7] Zachary F. Mainen & Terrence J. Sejnowski. “Influence of dendritic structure on firing pattern in model neocortical neurons.” In: [Nature](#) 382.6589 (1996). 00880, pp. 363–366.
- [8] Klas H. Pettersen & Gaute T. Einevoll. “Amplitude variability and extracellular low-pass filtering of neuronal spikes.” In: [Biophysical journal](#) 94.3 (2008). 00120, pp. 784–802.
- [9] David Sterratt et al. [Principles of computational modelling in neuroscience](#). 00081. 2011.